Nanoplasmonic Enhancement of Laser Energy Absorption

NAPLIFE 2022

T.S. Biró[1, 2, 3]

[1]NKFIH NAPLIFE national research program
Wigner Research Centre for Physics, Budapest

[2]Complex Science Hub, Vienna, Austria

[3]Babeş-Bolyai Egyetem, Cluj, Romania

Maribor, Slovenia, Xmas Symposium 2022 DEC. 15-17.

Energy mix

EU 2022 production

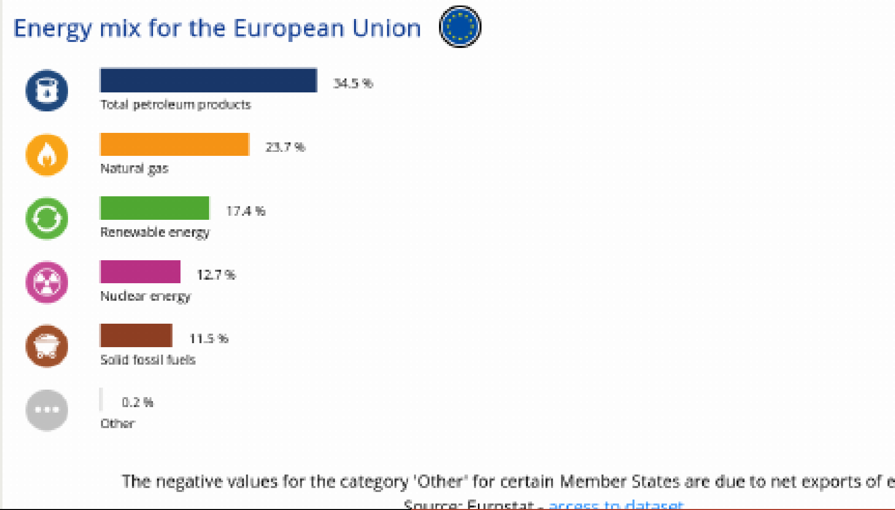

The negative values for the category 'Other' for certain Member States are due to net exports of e

Source: Eurostat - access to dataset

Energy prices for households

EU 2008 - 2022, HU 6,45 (2017) 9–18 (2022)

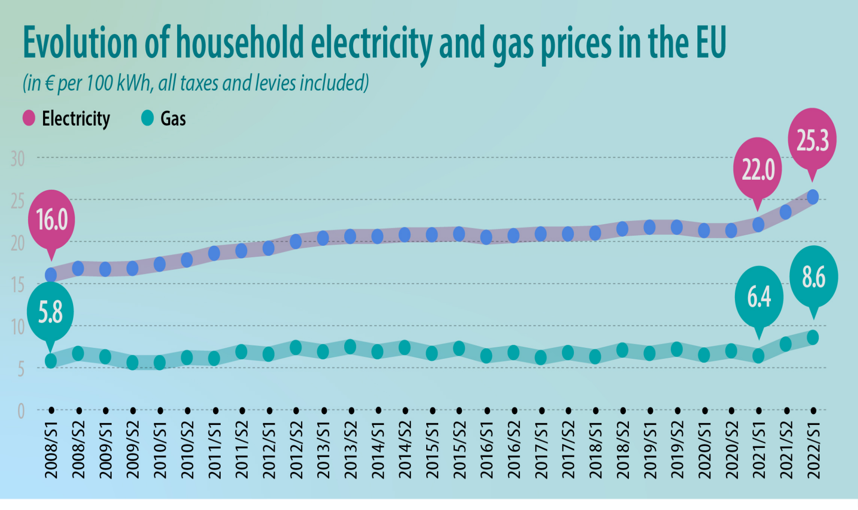

Hungarian electricity production (www.ksh.hu/stadat_files/ene/hu/

energy-mix (GWh)

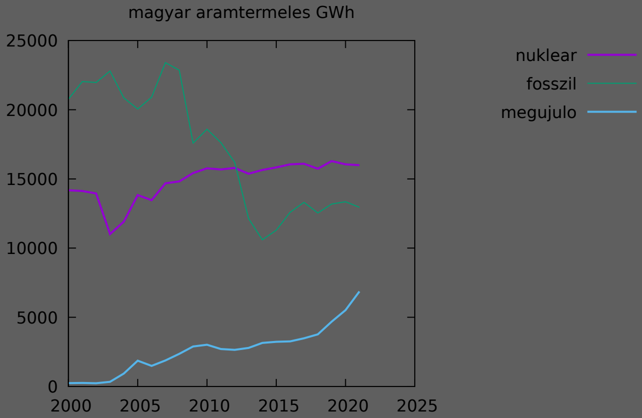

Reaction to the crisis

Summit


FUTURE OF UTILITIES

FUTURE OF UTILITIES
ENERGY TRANSITION SUMMIT

Europe's most significant energy conference

15 – 16 March 2023 | Amsterdam

Specific data, available energy

J/mg = MJ/kg

https://afdc.energy.gov/fuels/properties; https://en.wikipedia.org/wiki/energy_density

- coal 23; brown coal 18; turf 7; wood 11; biomass 10; hulladék 9; olajpala 20
- oil, PB gas 40; bio-fuel 30; waste 25
- natural gas 47; H 40; biogas 20; waste gas 15
- uranium 460.000; fusion 640.000.000

1 kg U $\approx$ 20 tons of coal $\approx$ 0.7 g fusion fuel

Specific energy content

need for logarithmic thinking

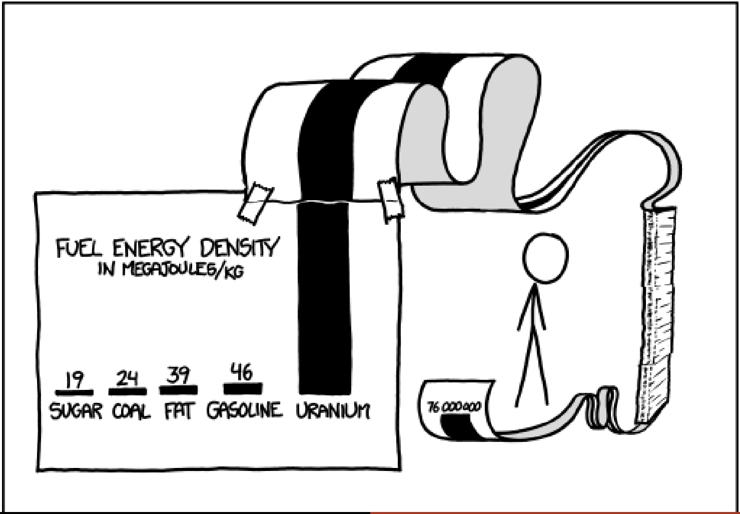

The ”atomic” force

nuclear techniques

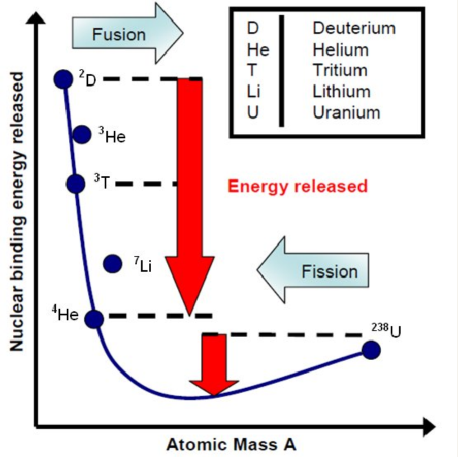

D	Deuterium
He	Helium
T	Tritium
Li	Lithium
U	Uranium

Thermal and equilibrium

ITER magnetic confinement

Direct and sudden

NIF laser shots

NIF

reactions and neutrons

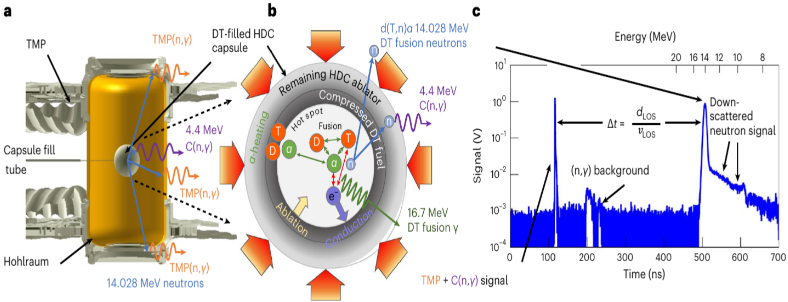

Fig. 1 | Indirect-drive inertial confinement fusion. a, Laser energy is converted into X-rays that compress and heat a spherical DT-filled capsule to generate fusion reactions. The HDC capsule is filled with DT gas through a fill tube and cryogenically frozen to create a solid DT ice layer on the inside surface. On heating and compression, the fusion of DT ions generates 14.028 MeV neutrons (blue) and γ-rays emitted by both fusion reaction and (n, γ) reactions in the surrounding capsule (purple) and the target TMP (orange). **b**, If heating of the compressed DT ice fuel by α-particles (green) emitted by the fusion reaction exceeds the radiation and electron conduction losses, the hot-spot reaction can become self-sustaining. **c**, The QCD nToF detectors on the NIF uniquely measure both γ- and neutron signals at approximately 100 and 500 ns, respectively. Low (n, γ) backgrounds enable a high-precision measurement of the mean line-of-sight neutron velocity v_{LOS} for a detector at distance d_{LOS}.

NIF

Announcements on achievments

$$Q = \frac{\text{energy out}}{\text{energy in}}$$

2021 August: Q = 0.7

2022 December 5-th: Q = 1.4

industry would need $Q \approx 300$

D + T fusion

why-s and problems

pictures from Rafelski

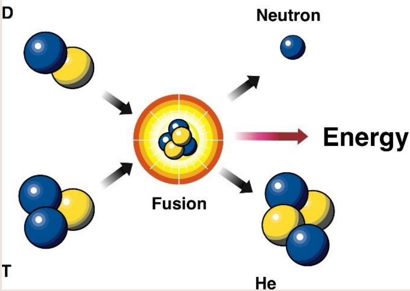

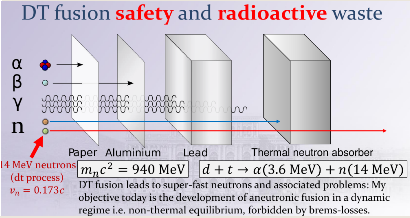

DT fusion **safety** and **radioactive** waste

14 MeV neutrons
(dt process)
$v_n = 0.173c$

$m_n c^2 = 940$ MeV

$d + t \to \alpha(3.6\ \mathrm{MeV}) + n(14\ \mathrm{MeV})$

DT fusion leads to super-fast neutrons and associated problems: My objective today is the development of aneutronic fusion in a dynamic regime i.e. non-thermal equilibrium, forbidden by brems-losses.

1. energetic neutrons; 2. global tritium quantity (nuclear power plants)

Neutronfree fusion

some reactions

However, the 0-generation plasma fusion reactor under construction is based on nuclear-weapon tritium cycle. My personal research interests are therefore today focused on fusion concepts that sidestep extreme density and temperature matter conditions required in the thermal equilibrium plasma devices, and the production of weapons-grade neutrons. I will introduce: Muon catalyzed cold nuclear fusion (not to be confounded with cold [con-]fusion); Laser driven proton acceleration induced micro-explosion fusion; and laser driven dynamical plasmon fusion. All three approaches are under active study, funded by both private and government sponsored research programs.

(Johann Rafelski, MTA inaugural talk, 2022. June 13.)

Neutronfree fusion

examples (wiki)

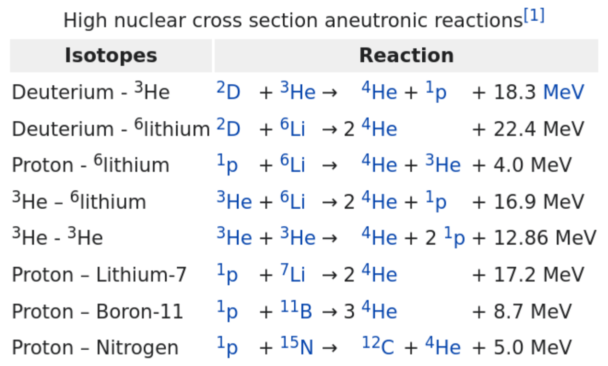

High nuclear cross section aneutronic reactions[1]

Isotopes	Reaction
Deuterium - ^{3}He	$^{2}\mathrm{D} + {}^{3}\mathrm{He} \rightarrow {}^{4}\mathrm{He} + {}^{1}\mathrm{p} + 18.3$ MeV
Deuterium - ^{6}lithium	$^{2}\mathrm{D} + {}^{6}\mathrm{Li} \rightarrow 2\,{}^{4}\mathrm{He} + 22.4$ MeV
Proton - ^{6}lithium	$^{1}\mathrm{p} + {}^{6}\mathrm{Li} \rightarrow {}^{4}\mathrm{He} + {}^{3}\mathrm{He} + 4.0$ MeV
^{3}He – ^{6}lithium	$^{3}\mathrm{He} + {}^{6}\mathrm{Li} \rightarrow 2\,{}^{4}\mathrm{He} + {}^{1}\mathrm{p} + 16.9$ MeV
^{3}He - ^{3}He	$^{3}\mathrm{He} + {}^{3}\mathrm{He} \rightarrow {}^{4}\mathrm{He} + 2\,{}^{1}\mathrm{p} + 12.86$ MeV
Proton – Lithium-7	$^{1}\mathrm{p} + {}^{7}\mathrm{Li} \rightarrow 2\,{}^{4}\mathrm{He} + 17.2$ MeV
Proton – Boron-11	$^{1}\mathrm{p} + {}^{11}\mathrm{B} \rightarrow 3\,{}^{4}\mathrm{He} + 8.7$ MeV
Proton – Nitrogen	$^{1}\mathrm{p} + {}^{15}\mathrm{N} \rightarrow {}^{12}\mathrm{C} + {}^{4}\mathrm{He} + 5.0$ MeV

Electrons in the fusion

PEP process, Widom-Larsen (wiki)

WL: $p + \boxed{e^-} \to n + \nu_e$ (-1.25 MeV), $p + n \to d + \gamma$ (+2.22 MeV)

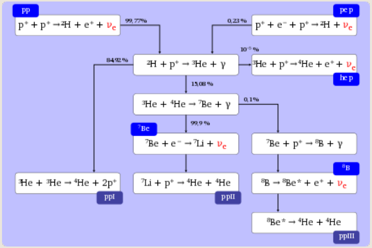

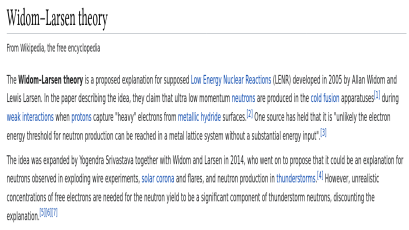

Widom-Larsen theory

From Wikipedia, the free encyclopedia

The **Widom-Larsen theory** is a proposed explanation for supposed Low Energy Nuclear Reactions (LENR) developed in 2005 by Allan Widom and Lewis Larsen. In the paper describing the idea, they claim that ultra low momentum neutrons are produced in the cold fusion apparatuses[1] during weak interactions when protons capture "heavy" electrons from metallic hydride surfaces.[2] One source has held that it is "unlikely the electron energy threshold for neutron production can be reached in a metal lattice system without a substantial energy input".[3]

The idea was expanded by Yogendra Srivastava together with Widom and Larsen in 2014, who went on to propose that it could be an explanation for neutrons observed in exploding wire experiments, solar corona and flares, and neutron production in thunderstorms.[4] However, unrealistic concentrations of free electrons are needed for the neutron yield to be a significant component of thunderstorm neutrons, discounting the explanation.[5][6][7]

NUclear fusion scales

in nature and in experiments

picture from Rafelski

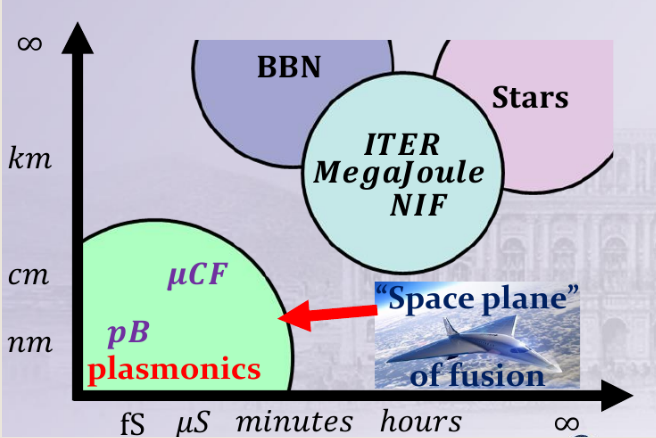

NAPLIFE individual features

Idea, plan, initial results

1. Plasmonic collectivity, energy concentration, threshold lowering, lifetime cca. 20 – 30 fs
2. Far from equilibrium, lightspeed, simultaneous ignitions
3. Nanoantennas in target, ultrashort, high contrast laser pulses (10^6, 40 fs @ Wigner)
4. Energy balance and fusion products at low energy: microcraters, D/(2D+H)

NAPLIFE

laser board and vacuum chamber

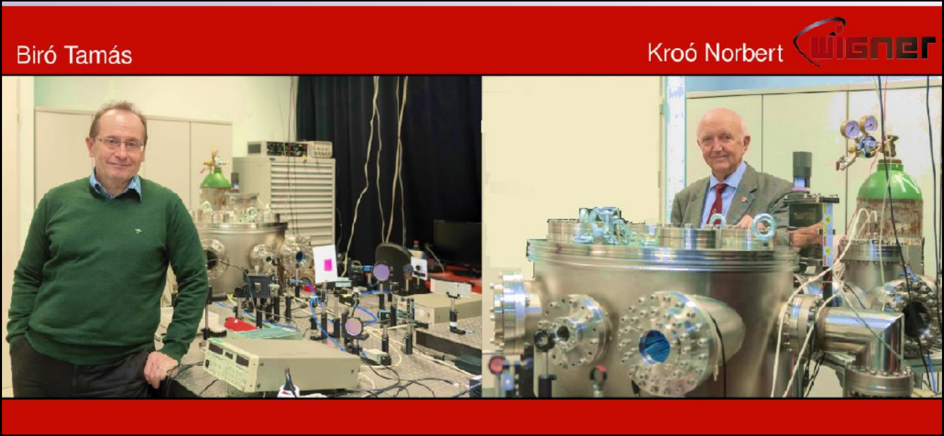

Lab Structure

organogram

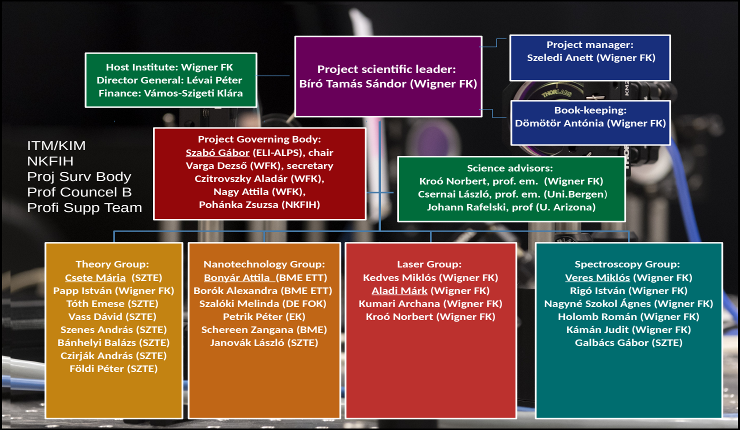

Host Institute: Wigner FK
Director General: Lévai Péter
Finance: Vámos-Szigeti Klára

Project scientific leader:
Bíró Tamás Sándor (Wigner FK)

Project manager:
Szeledi Anett (Wigner FK)

Book-keeping:
Dömötör Antónia (Wigner FK)

ITM/KIM
NKFIH
Proj Surv Body
Prof Councel B
Profi Supp Team

Project Governing Body:
Szabó Gábor (ELI-ALPS), chair
Varga Dezső (WFK), secretary
Czitrovszky Aladár (WFK),
Nagy Attila (WFK),
Pohánka Zsuzsa (NKFIH)

Science advisors:
Kroó Norbert, prof. em. (Wigner FK)
Csernai László, prof. em. (Uni.Bergen)
Johann Rafelski, prof (U. Arizona)

Theory Group:
Csete Mária (SZTE)
Papp István (Wigner FK)
Tóth Emese (SZTE)
Vass Dávid (SZTE)
Szenes András (SZTE)
Bánhelyi Balázs (SZTE)
Czirják András (SZTE)
Földi Péter (SZTE)

Nanotechnology Group:
Bonyár Attila (BME ETT)
Borók Alexandra (BME ETT)
Szalóki Melinda (DE FOK)
Petrik Péter (EK)
Schereen Zangana (BME)
Janovák László (SZTE)

Laser Group:
Kedves Miklós (Wigner FK)
Aladi Márk (Wigner FK)
Kumari Archana (Wigner FK)
Kroó Norbert (Wigner FK)

Spectroscopy Group:
Veres Miklós (Wigner FK)
Rigó István (Wigner FK)
Nagyné Szokol Ágnes (Wigner FK)
Holomb Román (Wigner FK)
Kámán Judit (Wigner FK)
Galbács Gábor (SZTE)

Group Structure

cooperation

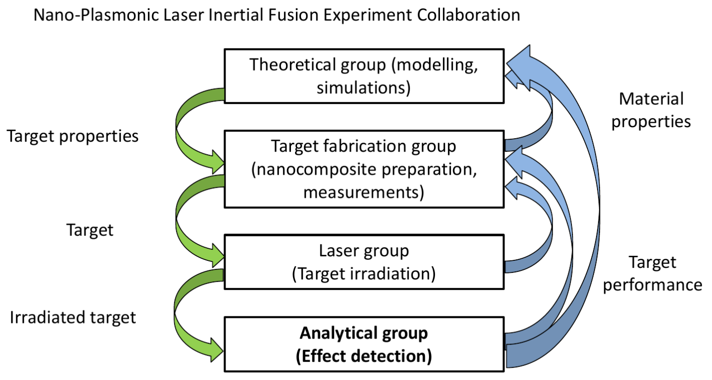

Nano-Plasmonic Laser Inertial Fusion Experiment Collaboration

Theoretical group (modelling, simulations)

Target fabrication group (nanocomposite preparation, measurements)

Laser group (Target irradiation)

Analytical group (Effect detection)

Nanofusion

plasmons: barrier reduced, energy hot spots

The Lycurgus Cup
A Roman
Nanotechnology

Ian Freestone[1], Nigel Meeks[2],
Margaret Sax[2] and Catherine Higgitt[2]

Transmission electron microscopy (TEM) image of a silver-gold alloy particle within the glass of the Lycurgus Cup

The Lycurgus Cup *1958,1202.1 in reflected (a) and transmitted (b) light. Scene showing Lycurgus being enmeshed by Ambrosia*

Fusion cross section

when electrons screen the Coulomb barrier (Wong+Shih 2022)

Formula $\sigma(E, U_s) = \frac{S(E+U_s)}{E+U_s}\left[e^{\pi\sqrt{2.29\mathrm{MeV}/(E+U_s)}} - 1\right]^{-1}.$

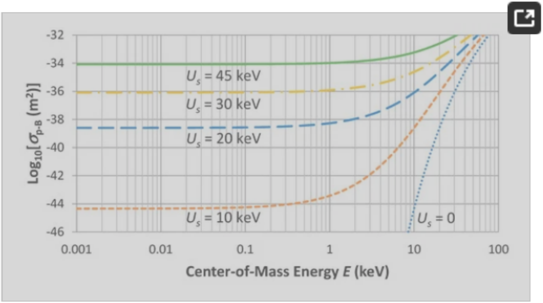

Figure 1. p-^{11}B cross section as function of particle energy for the screening electron densities up to U_s = 45 keV. The cross section below ***E*** = 1 keV grows over 10 orders of magnitude (from 10^{-44} to 10^{-34} m^2) when U_s increases from 10 to 45 keV.

Plasmonics at work

nanoplasmonics simulations (M. Csete)

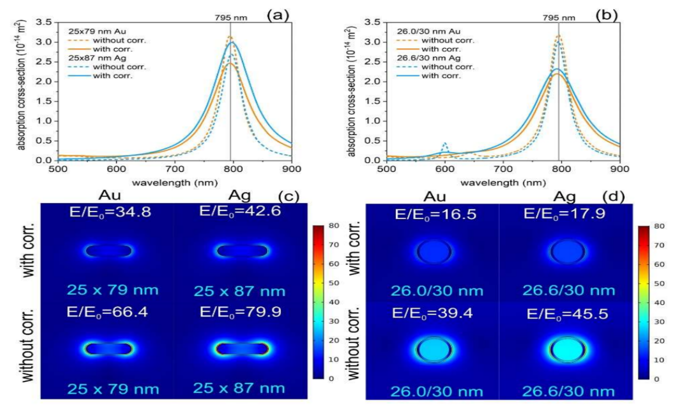

Plasmonics at work

near field enhancement (M. Csete)

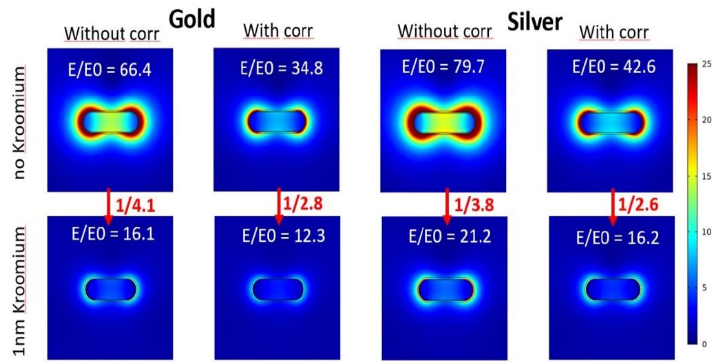

1.1.2. ábra A vizsgált rendszerek közeltér erősítés eloszlása ($|\mathbf{E}|/|\mathbf{E}_0|$).

Plasmonics at work

polluted nanoantennas (M. Csete)

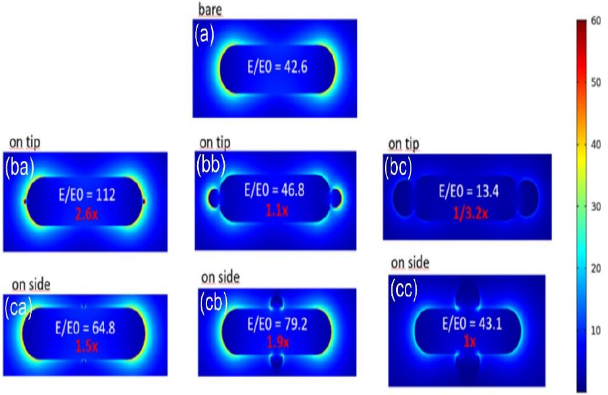

1.1.5. ábra A vizsgált ezüst (korrigált $\varepsilon(\omega)$ függvény) rendszerek közeltér erősítés eloszlása ($|\mathbf{E}|/|\mathbf{E}_0|$). (a) Kroómium nélküli eset, (ba-bc) on-apex és (ca-cc) on-side konfigurációk 1 nm – 10 nm KNP mérettel.

Plasmonics at work

nanoantenna form variations (M. Csete)

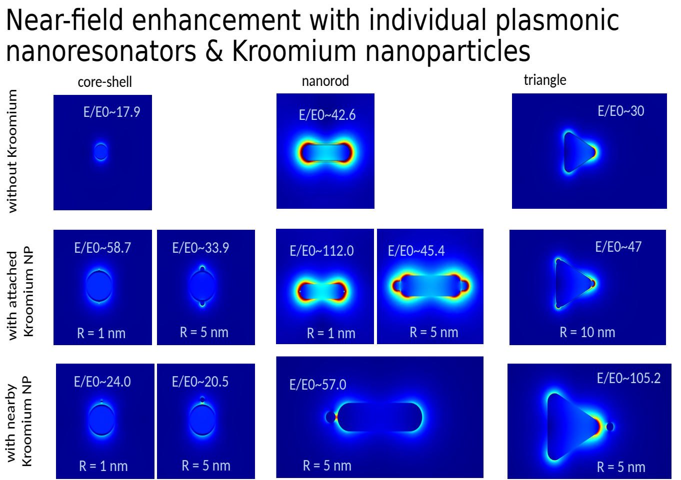

Near-field enhancement with individual plasmonic nanoresonators & Kroomium nanoparticles

Kinetic model: PIC

Single nanorod momentum distributions (I. Papp)

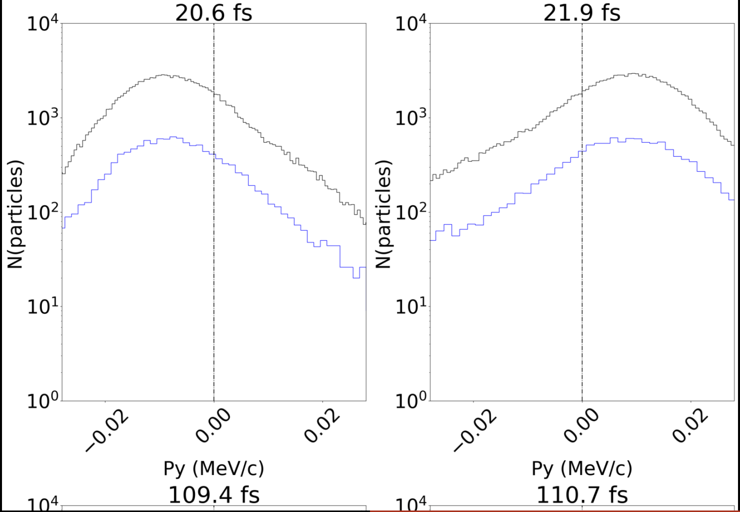

Kinetic model: PIC

Single nanorod

Compare vacuum to UDMA (I. Papp)

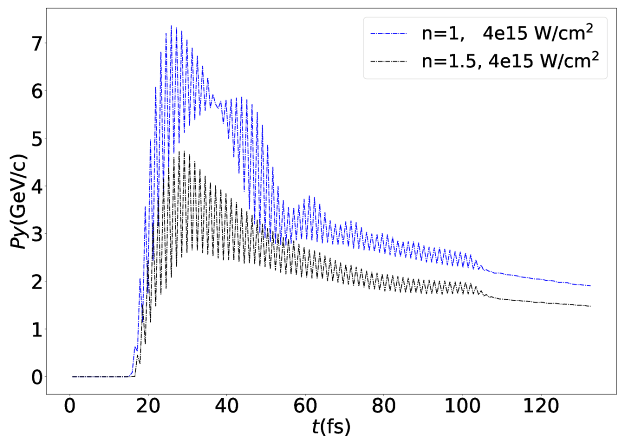

Kinetic model: PIC

Single nanorod time evolution (I. Papp)

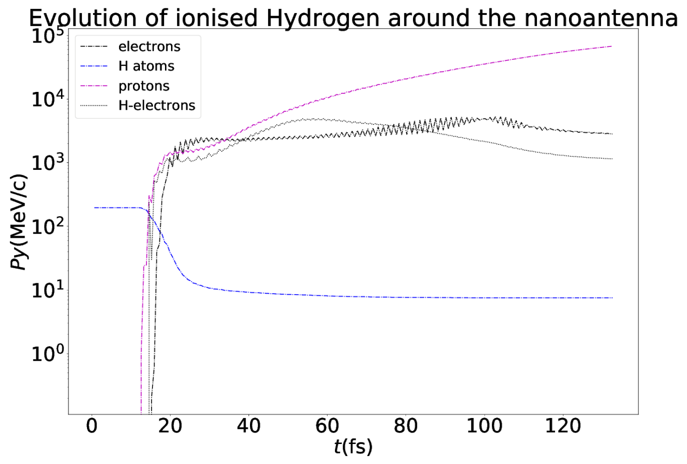

NAPLIFE (25 mJ, 40 fs) vs NIF (1 MJ, 10 ns)

Rapid and slow ignition (L. Csernai)

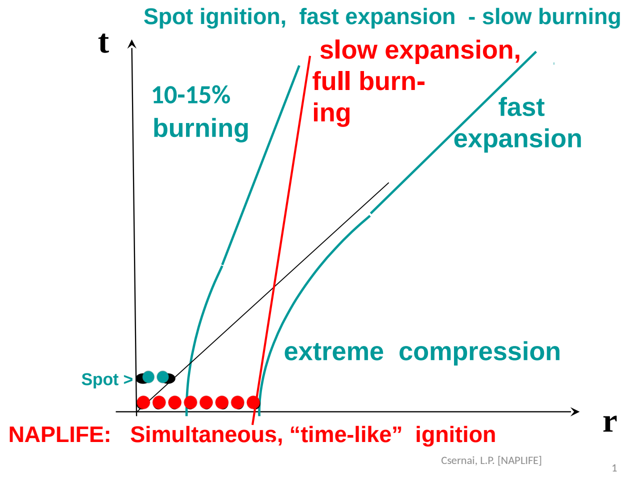

Spot ignition, fast expansion - slow burning

slow expansion, full burn-ing

10-15% burning

fast expansion

extreme compression

NAPLIFE: Simultaneous, “time-like” ignition

Csernai, L.P. [NAPLIFE]

NAPLIFE NANO

Au nanorods microscopic image, absorption curve (Bonyár)

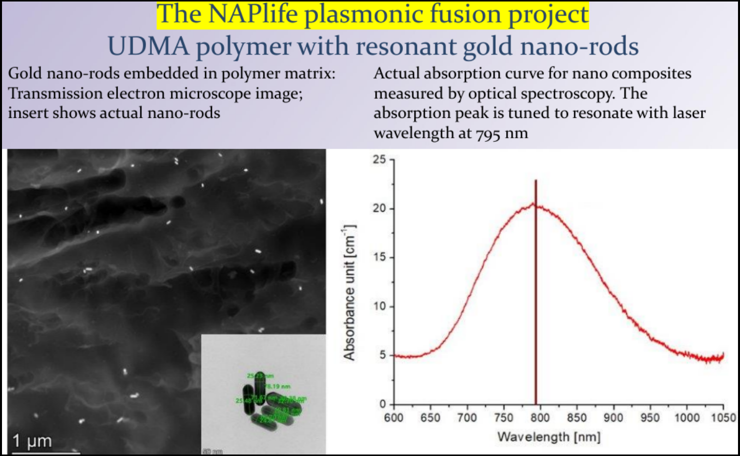

The NAPlife plasmonic fusion project

UDMA polymer with resonant gold nano-rods

Gold nano-rods embedded in polymer matrix: Transmission electron microscope image; insert shows actual nano-rods

Actual absorption curve for nano composites measured by optical spectroscopy. The absorption peak is tuned to resonate with laser wavelength at 795 nm

NAPLIFE NANO

Scattered nanorod patterns (Bonyár, Veres)

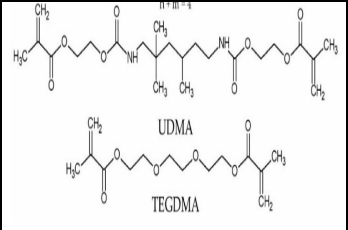

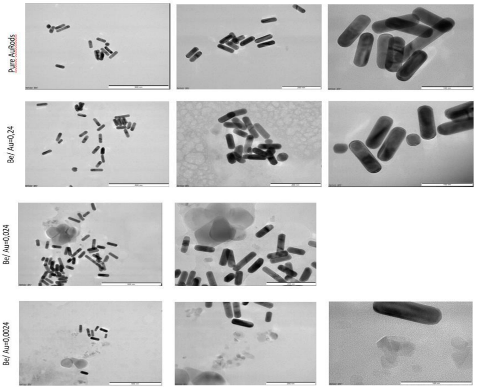

12. ábra. A különböző AuRods/ Be aránnyal rendelkező minták TEM felvételei

NAPLIFE CRATER

craters’ scanning electro microscope images (J. Kámán)

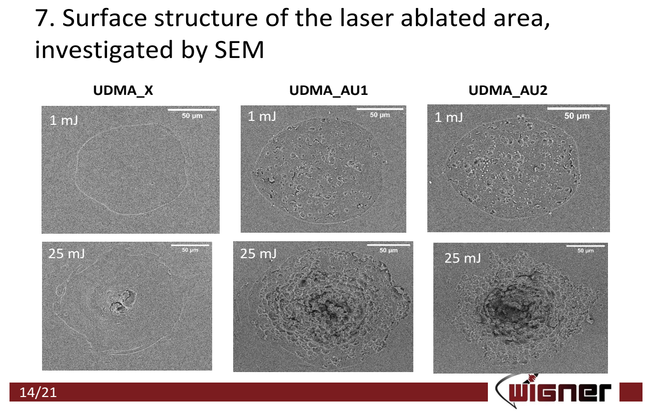

7. Surface structure of the laser ablated area, investigated by SEM

UDMA_X **UDMA_AU1** **UDMA_AU2**

14/21

NAPLIFE CRATER

microcraters in craters (J. Kámán)

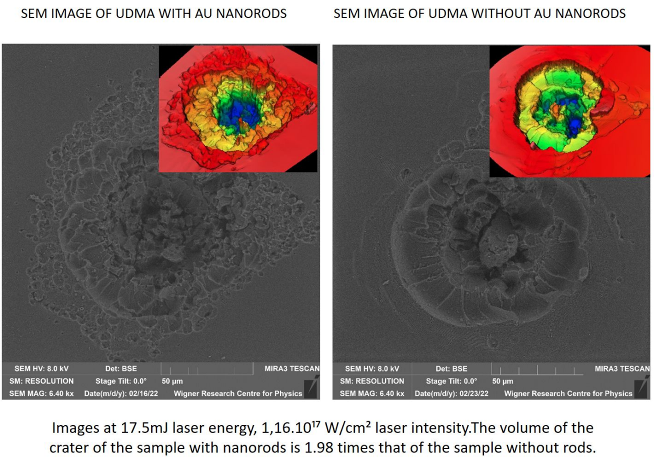

SEM IMAGE OF UDMA WITH AU NANORODS

SEM IMAGE OF UDMA WITHOUT AU NANORODS

Images at 17.5mJ laser energy, $1{,}16.10^{17}$ W/cm^2 laser intensity.The volume of the crater of the sample with nanorods is 1.98 times that of the sample without rods.

NAPLIFE CRATER

microcrater contours (J. Kámán)

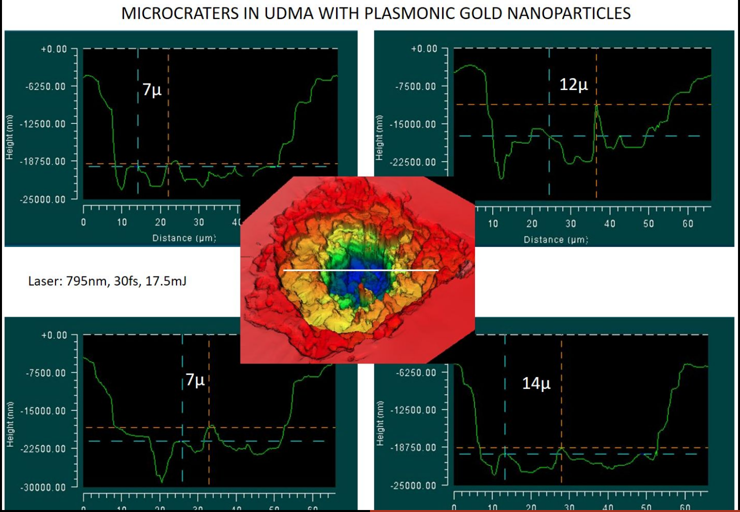

MICROCRATERS IN UDMA WITH PLASMONIC GOLD NANOPARTICLES

Laser: 795nm, 30fs, 17.5mJ

NAPLIFE CRATER

shot craters (Á. Nagyné Szokol)

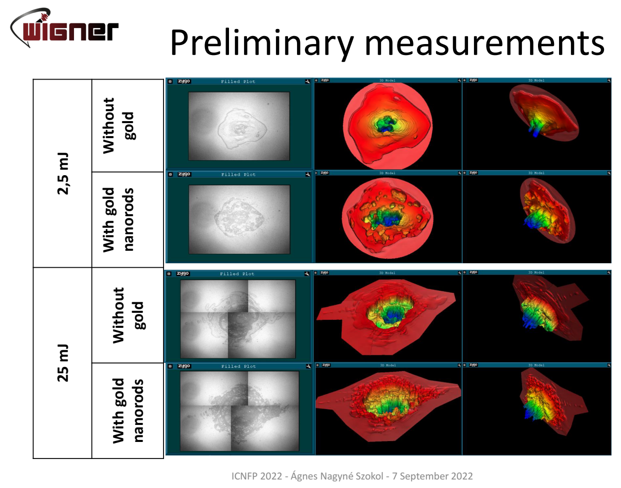

Preliminary measurements

2,5 mJ	Without gold	
	With gold nanorods	
25 mJ	Without gold	
	With gold nanorods	

ICNFP 2022 - Ágnes Nagyné Szokol - 7 September 2022

NAPLIFE CRATER

Craters w/o Au

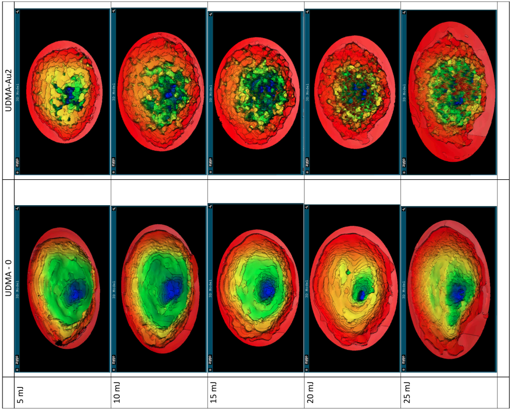

12. ábra: A Spektroszkópia csoport Zygo interferométerrel végzett mérési eredményei a belövési kráterekről UDMA-Au0, valamint UDMA-Au2 mintákról 5-25 mJ impulzusenergiák között.

NAPLIFE CRATER

method to obtain the crater volume (Á. Nagyné Szokol)

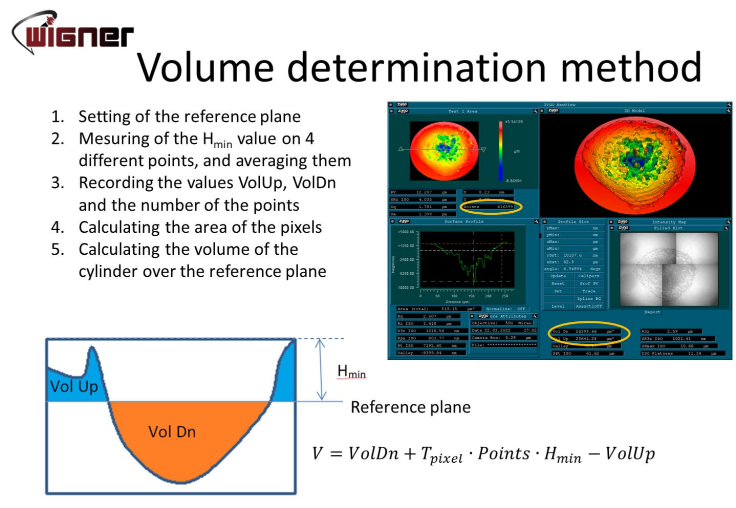

Volume determination method

1. Setting of the reference plane
2. Mesuring of the H_{min} value on 4 different points, and averaging them
3. Recording the values VolUp, VolDn and the number of the points
4. Calculating the area of the pixels
5. Calculating the volume of the cylinder over the reference plane

PV 12.207 µm
SRz ISO 4.035 µm
Sq 1.781 µm
Sa 1.399 µm
X 0.23 mm
Points 416399

yDst: 10107.6 nm
xDst: 82.9 µm
angle: 6.94894 degs

Area (total) 519.15 µm²
Normalize: Off
Rq 2.607 µm
Rz ISO 3.418 µm
R3z ISO 1010.56 nm
Rpm ISO 803.77 nm
Pt ISO 7195.60 nm
Valley -8399.84 nm

Objective: 50X Mirau
Date 22.03.2022 17:02
Camera Res: 0.29 µm
File: ******************

Vol Dn 26399.66 µm³
Vol Up 23641.28 µm³
SPt ISO 61.62 µm

R3z 2.59 µm
SR3z ISO 1021.41 nm
SRmax ISO 10.66 µm
ISO Flatness 11.34 µm

$$V = VolDn + T_{pixel} \cdot Points \cdot H_{min} - VolUp$$

NAPLIFE CRATER

crater volumes vs pulse energy (Á. Nagyné Szokol)

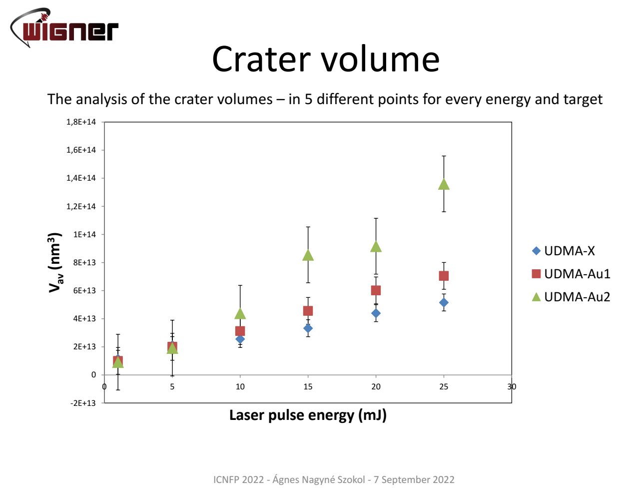

Crater volume

The analysis of the crater volumes – in 5 different points for every energy and target

ICNFP 2022 - Ágnes Nagyné Szokol - 7 September 2022

NAPLIFE RAMAN

UDMA - TEGDMA copolymer (Veres)

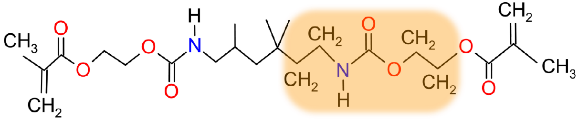

Figure 1. Chemical structure of UDMA monomer together with the selected part used for further modeling and calculations.

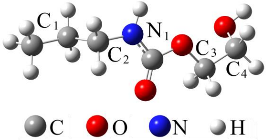

Figure 2. Optimized (B3LYP/6-311++G(d,p)) geometry of UDMA model (C_1H_2-C_2H_2 and C_3H_2-C_4H_2 groups are in anti and gauche conformational states, respectively).

NAPLIFE RAMAN

Raman signals: vibration of molecular bonds (Veres)

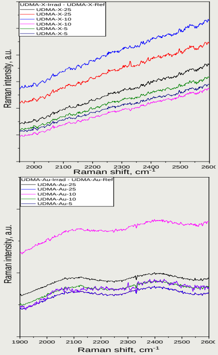

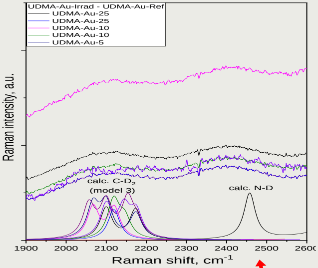

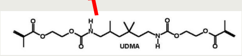

$I_{laser} > 10^{16}$

NAPLIFE RAMAN

Raman signals: molecular vibrations from various spots in teh crater

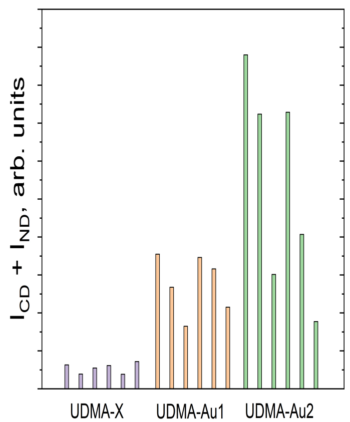

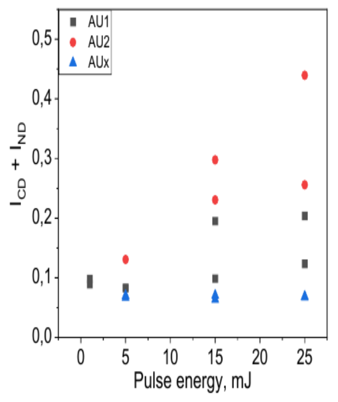

NAPLIFE LIBS

LIBS: plasma plum (Aladi)

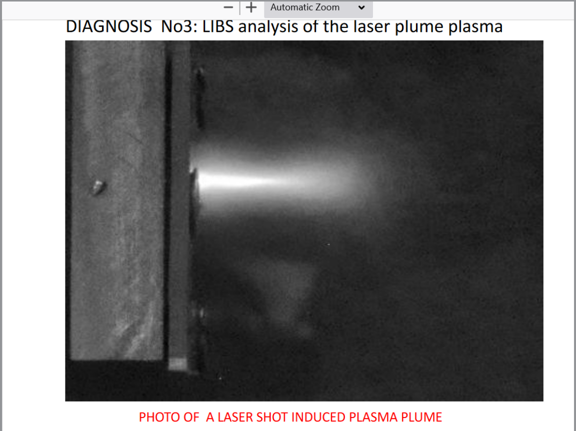

DIAGNOSIS No3: LIBS analysis of the laser plume plasma

PHOTO OF A LASER SHOT INDUCED PLASMA PLUME

NAPLIFE LIBS

LIBS: atomic ionisation → D/H (Aladi)

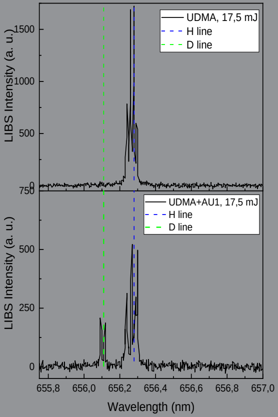

NAPLIFE LIBS+

LIBS: spectral areas → D/(2D+H) (Kroó)

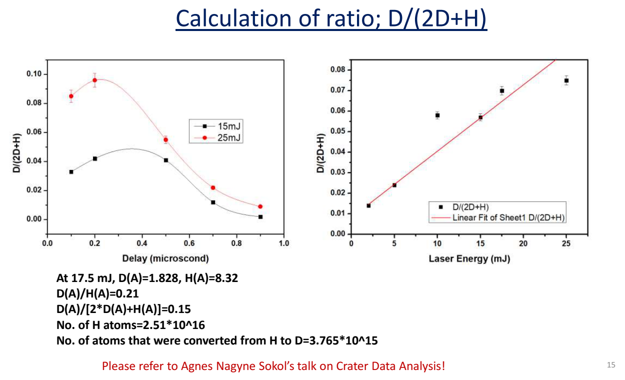

Calculation of ratio; D/(2D+H)

At 17.5 mJ, D(A)=1.828, H(A)=8.32
D(A)/H(A)=0.21
D(A)/[2*D(A)+H(A)]=0.15
No. of H atoms=2.51*10^16
No. of atoms that were converted from H to D=3.765*10^15

Please refer to Agnes Nagyne Sokol's talk on Crater Data Analysis!

NAPLIFE LIBS++

LIBS: kinetic energy estimate (Kroó, Biró)

Delay times → velocity distribution (rough proxy)

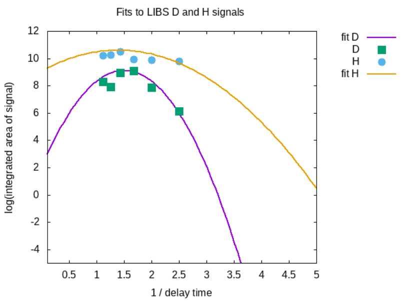

$$t_{max} \approx 0.6\ \mu\ \mathrm{s},\ t_{light} \approx 0.13\ \mathrm{ns},\ t_{2\to 3} \approx 2\ \mathrm{fs}.$$

$$v_D \approx 70\ \mathrm{km/s},\ E_{D,kin} \approx 50\ \mathrm{eV}, \qquad \frac{v_D}{c} \approx 2 \cdot 10^{-4}.$$

NAPLIFE NUC

compare to $p+n \to d+\gamma$ (Biró + Jakovác)

In p and n CMS, no barrier, $v_p = v_n = 0$ approximation $\to$ $|p_D| = |p_\gamma| = E_\gamma/c$.

$$m_p c^2 + m_n c^2 = m_D c^2 + \frac{|p_D|^2}{2m_D} + c|p_D|,$$

The deuteron binding energy dominates:
$B = m_p c^2 + m_n c^2 - m_D c^2 \approx 2.2$ MeV

since it is much less than $m_D c^2 \approx 2$ GeV, practically

$$\frac{v_D}{c} \approx \frac{B}{m_D c^2} \approx 1.1 \cdot 10^{-3}.$$

NAPLIFE MASS SPECTRO

mass spectrometer peaks: amu1 300, amu2 230.000, amu3 17.500, amu4 100 (Aladi)

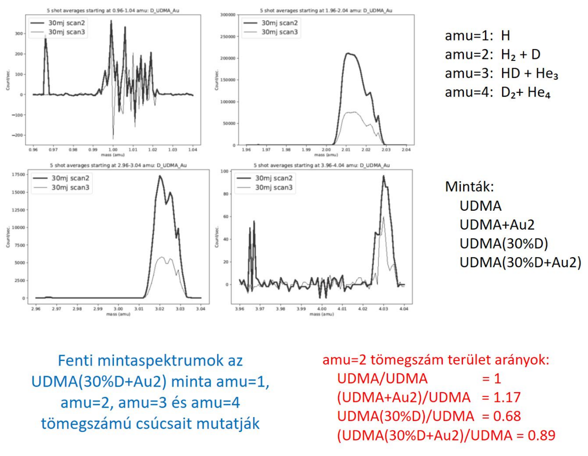

amu=1: H
amu=2: H_2 + D
amu=3: HD + He_3
amu=4: D_2+ He_4

Minták:
- UDMA
- UDMA+Au2
- UDMA(30%D)
- UDMA(30%D+Au2)

Fenti mintaspektrumok az UDMA(30%D+Au2) minta amu=1, amu=2, amu=3 és amu=4 tömegszámú csúcsait mutatják

amu=2 tömegszám terület arányok:
UDMA/UDMA = 1
(UDMA+Au2)/UDMA = 1.17
UDMA(30%D)/UDMA = 0.68
(UDMA(30%D+Au2)/UDMA = 0.89

ENERGY: transmitted light $<$ 2 %

M. Kedves

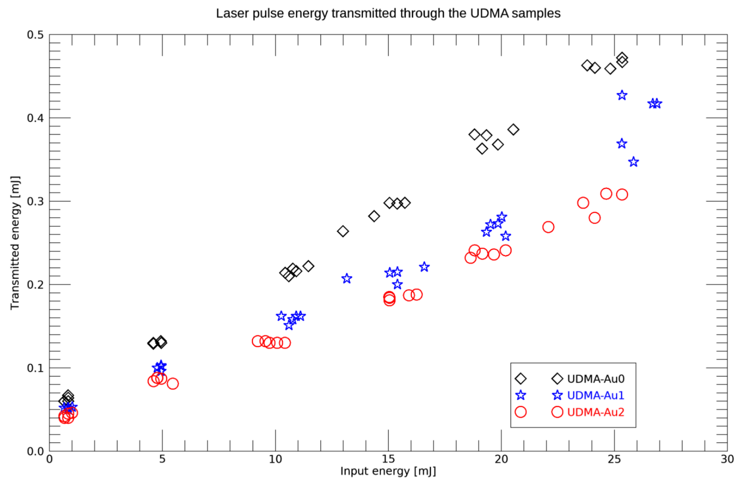

ENERGY: 17.5 mJ → 3.3 J: Q = 188 ?

Estimate the energy affairs

N. Kroó

velocities from LIBS delays: $v \approx 70$ km/s

Kinetic energy of a single deuteron:

$$E_{\mathrm{kin,D}} = \frac{1}{2} mc^2 \frac{v^2}{c^2} \approx 53 \text{ eV} \approx 8,5 \cdot 10^{-18} \text{ J}.$$

Number of deuterons from crater sizes: $N_D \approx 1,68 \cdot 10^{15}$

Total energy for UDMA amu (470):

$$\frac{1}{2} m_{\mathrm{UDMA}} v^2 = \frac{amu}{2} E_{\mathrm{kin,D}} \approx 3,3 \text{ J}.$$

$Q = 3.3$ **J** / 17.4 **mJ** ≈ 188

NAPLIFE FUTURE

plans and suggestions

Our proosal to NKFIH (March 30, May 31, June 30; approvement October 30)

Our further plans:

- Nuclear detection (CR39)
- ELI cooperation (similar and bigger lasers)
- Variation of the shooting geometry
- Nanoparticles and medium matter variations
- energy, deuteron and α observation